Aerosol water parameterization: long-term evaluation and importance

—

Supplemental Material

S. Metzger et al.,

June 4, 2018

S1 Complementary results

This section extends/complements the applications shown in Sec. 3 and 4 (main text):

1. EMAC AOD versus AERONET and Satellites
   see Sec. S1.1 and Sec. 3.1 (main text)
2. EQSAM4clim versus ISORROPIA II for 2000–2013
   see Sec. S1.2 and Sec. 3.2 (main text)
3. EQSAM4clim versus ISORROPIA II for 2005
   see Sec. S1.3 and Sec. 3.3 (main text)

AERONET/EMEP stations

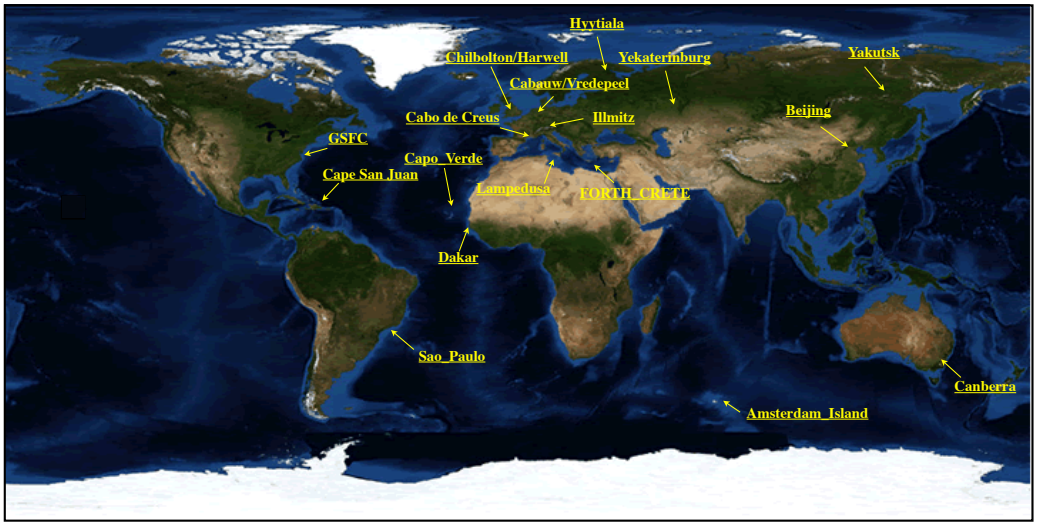

AERONET - http://aeronet.gsfc.nasa.gov/cgi-bin/type_piece_of_map_opera_v2_new **EMEP** - http://ebas.nilu.no/default.aspx

Amsterdam_Island (37S,77E)	Sao_Paulo (23S,46W)	Dakar (14N,16W)	Cabauw (51N,4E)	Lampedusa (35N,12E)	Yekaterinburg (57N,59E)	Beijing (39N,116E)
GSFC (38N,76W)	Cape_San_Juan (18N,65W)	Capo_Verde (16N,22W)	Chilbolton (51N,1W)	FORTH_CRETE (35N,25E)	Yakutsk (61N,129E)	Canberra (35S,149E)
EMEP	Cabo de Creus (42N,3E)	Vredepeel (51N,4E)	Harwell (51N,1W)	Cabauw (51N,4E)	Illmitz (48N,16E)	Hyytiala (61N,24E)

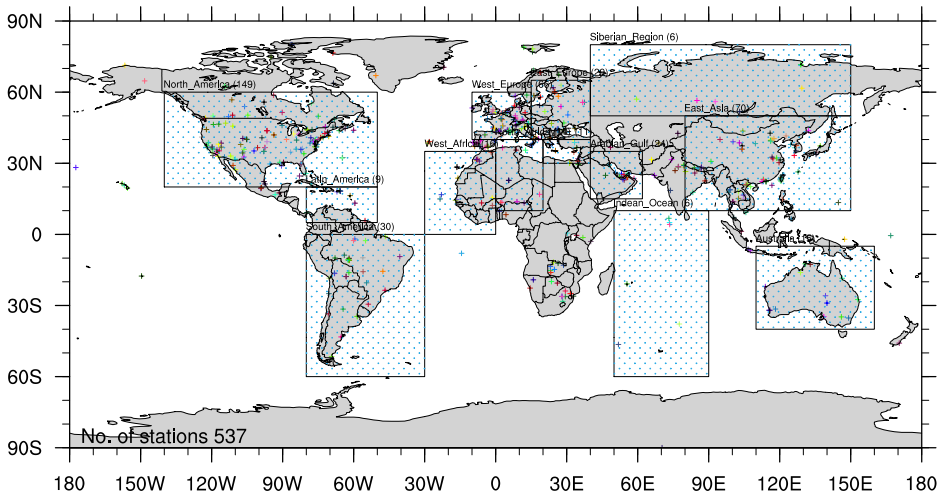

Figure S1: (Top) Locations of selected AERONET and EMEP stations used (main text), (bottom) all 537 AERONET station locations representing 14 regions of the Earth used for the statistics of our EMAC evaluation study (e.g., Scatter plots in this Supplement).

S1.1 EMAC AOD versus AERONET and Satellites

Figure S2–S4 complement Fig. 2 (main text) and shows the AOD results of our EMAC model version (Sec. 2) based on EQSAM4clim and ISORROPIA II in comparison to the results of Pozzer et al. (2015) (PO2015) for the period 2000-2010.

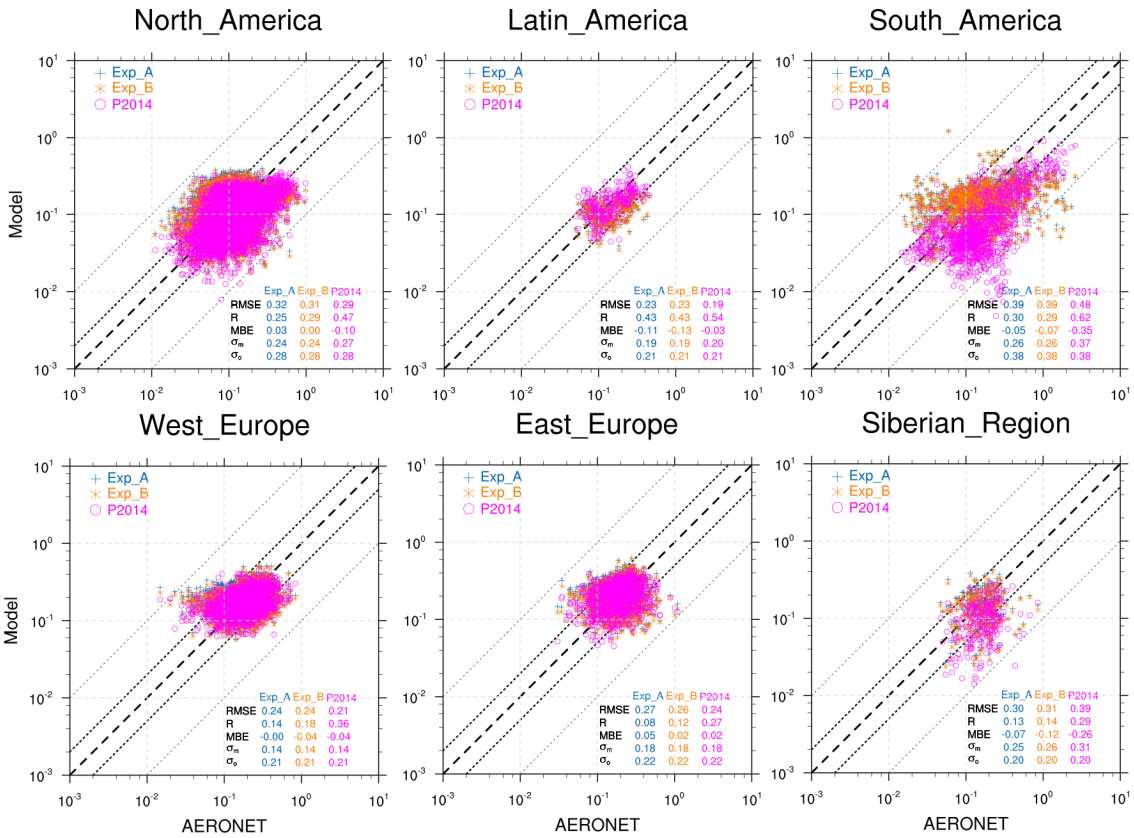

Figure S2: Scatter plots for the EMAC model AOD (2000-2010 mean): ISORROPIA II (blue stars) and EQSAM4clim (orange circles) and Pozzer et al. (2015) (pink crosses) versus 537 AERONET observations shown in Fig. S1. The results support Figs. 2 and 3 that are shown in the main text.

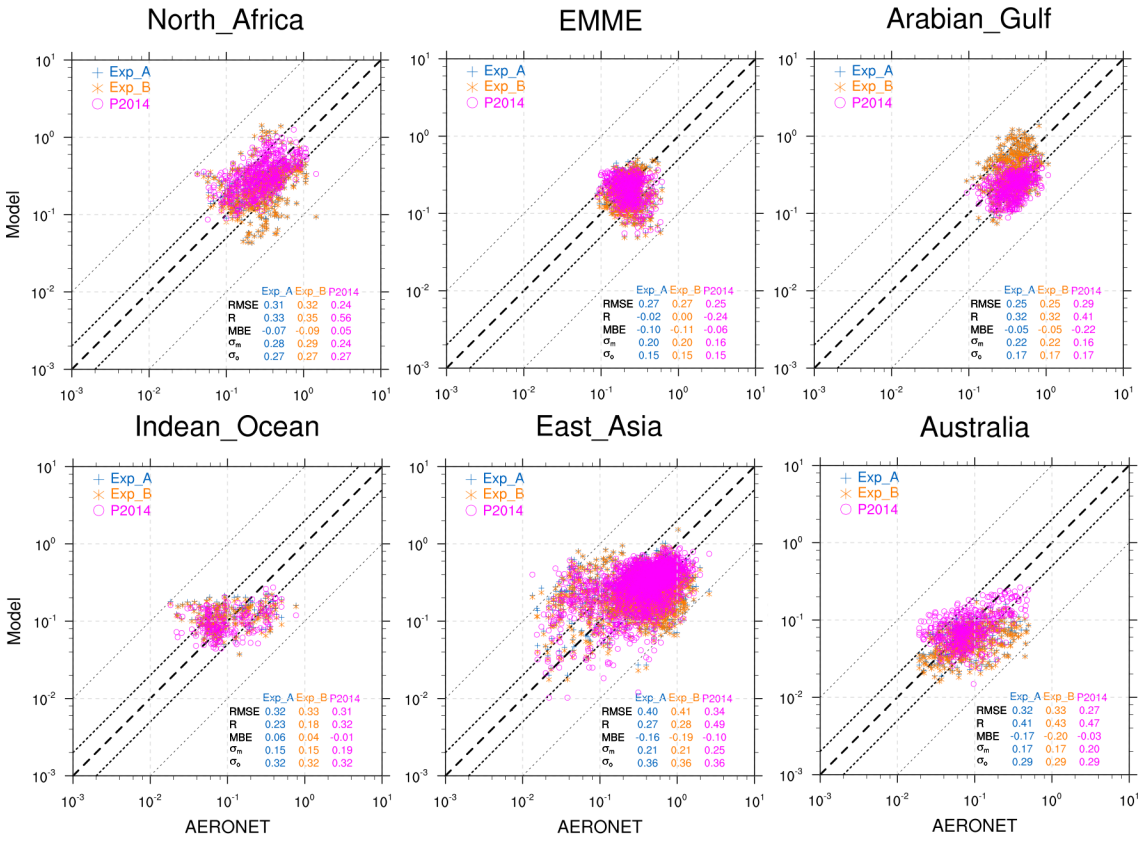

Figure S3: Fig. S2 continued.

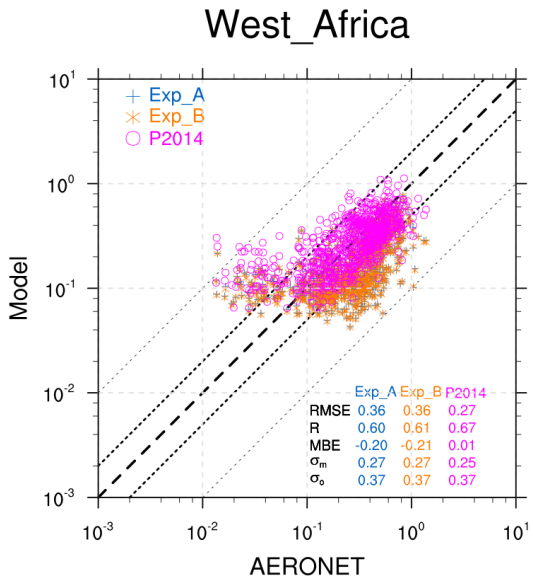

Figure S4: Fig. S2 continued.

S1.2 EQSAM4clim versus ISORROPIA II for 2000–2013

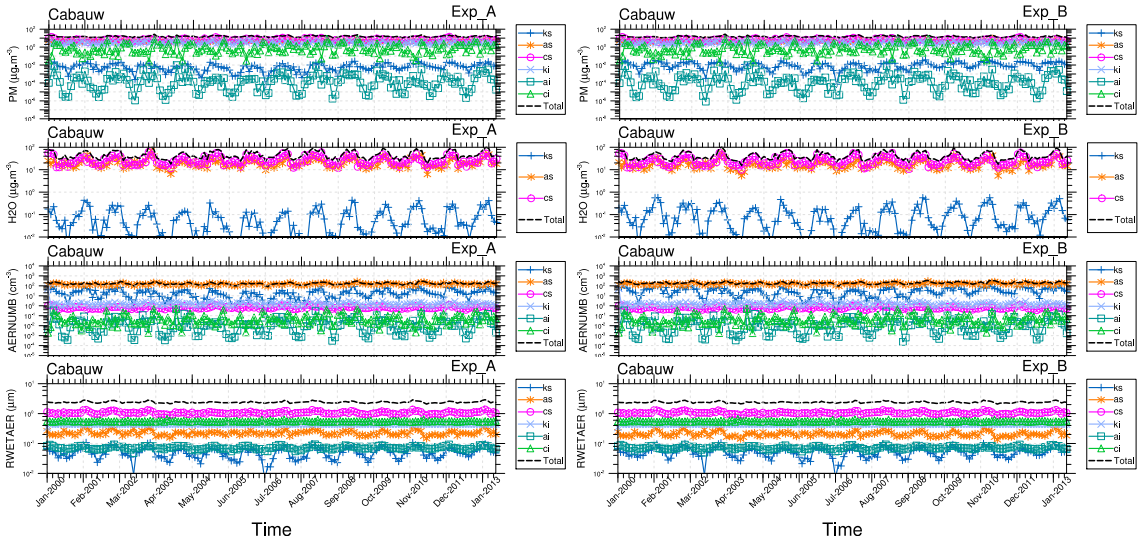

Figure S5: Various aerosol properties at the EMEP site Cabauw for the period 2000-2013: PM (top row) and H_2O (2nd row), aerosol number concentration (3rd row), aerosol wet radius (bottom row), including each aerosol mode: nucleation soluble (ns), aitken soluble (ks), accumulation soluble (as), coarse soluble (cs), aitken insoluble (ki), accumulation insoluble (ai), coarse insoluble (ci), sum of all modes (total). ISORROPIA II (left column) and EQSAM4clim (right column). This Figure complements Figure 5 (main text).

S1.3 EQSAM4clim versus ISORROPIA II for 2005

The following results complement our model comparison discussed in Sec. 4.1 (main text). Note that differences in this comparison are most sensitive to the water uptake calculation approaches of EQSAM4clim and ISORROPIA II. Figures S6 and S7 show the EMAC results of the total aerosol PM and water for our selection of AERONET sites (Fig. 1). Figures S8–S16 show the corresponding EMAC tracers (all monthly means based on a 5 hourly output), i.e., lumped aerosol sulfate, bi-sulfate, nitrate, chloride, ammonium, sodium, potassium, magnesium and calcium [$\mu g/m^3$(air)]. Each station shows the tracer masses (sum of all modes) of two identical "no aging" EMAC simulations based on EQSAM4clim and ISORROPIA II. Figures S17–S20 show the corresponding scatter plots. Each scatter plot shows annual means for key (three soluble) aerosol modes of GMXe (Sec. 2.2): coarse (top row), accumulation (middle row) and aitken (bottom row). Fig. S17 shows the total aerosol mass (PM) and water (H_2O) plus growth factor (GF); Fig. S18 shows potassium (K^+), magnesium (Mg^{2+}) and calcium (Ca^{2+}); Fig. S19 shows sulfate ($SO_4{}^{2-}$), bi-sulfate ($HSO_4{}^-$) and sodium (Na^+); Fig. S20 shows ammonium ($NH_4{}^+$), nitrate ($NO_3{}^-$) and chloride (Cl^-). Each panel includes the statistics: Root Mean Square Error ($RMSE$), Correlation Coefficient (R), Mean biased Error (MBE), Standard deviation of ISORROPIA II (x-STD) and EQSAM4clim (y-STD). Note Table 3 (main text) which complements the time series and scatter plots with the corresponding statistics of various EMAC tracers (sum over all modes, annual mean and station mean) based on the 537 stations shown in Fig. S1.

The size-segregated scatter plots (Fig. S17–S20) support the time series and station analysis. The EMAC results of all non-volatile compounds, except bi-sulfate, are very close for both schemes. Especially the non-volatile cations and anions (Figs. S18–S19) are all close to the one-to-one lines (dashed) for all modes. Only ammonium (Fig. S20), which is the only volatile cation considered in our EMAC applications, shows more scatter in the aitken mode as a result of differences in the associated bi-sulfate predictions (Fig. S19). The volatile anions, nitrate and chlorine, also show some scatter which increases with decreasing aerosol radius (Fig. S20), but the differences are rather small and for most cases within the two-by-two lines (dotted). The increasing differences with decreasing aerosol size is also reflected in the aerosol water mass results (Fig. S17). This is expected, since we consider here the Kelvin-term for EQSAM4clim (see Eq. A7 in Metzger et al., 2016a), which is not the case for ISORROPIA II. The Kelvin effect accounts for an increase of vapor pressure above the droplet surface with decreasing particle size and therefore leads to less water uptake compared to bulk (size-independent) calculations. The effect is, however, only noticeable for aitken mode particles and smaller, those mass concentrations are generally negligible small, particularly for the total aerosol water mass. Note that the GF is much less sensitive to difference compared to the water mass due to the power of one-third (see e.g., Eq. A8 in Metzger et al., 2016a). This is one reason why we focus on the aerosol water for our hygroscopic growth evaluation of EQSAM4clim.

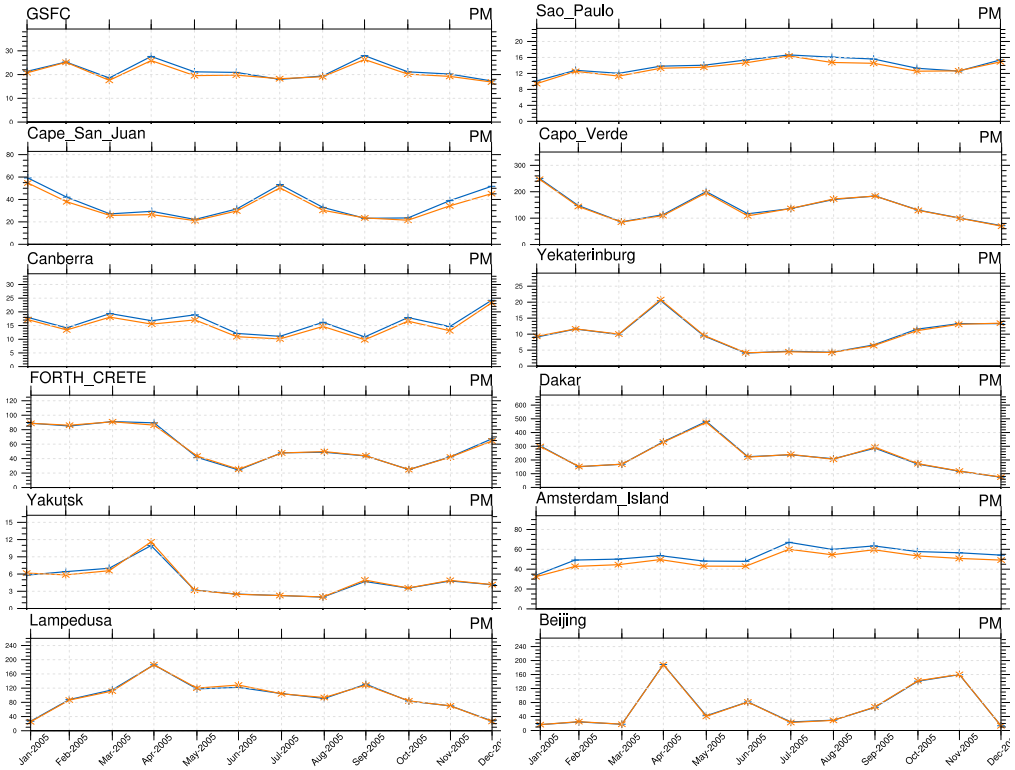

Figure S6: Selected time-series of the total (sum of all aerosol modes) particulate matter (PM) (excluding aerosol water) for 2005 (monthly means) representing the different regions of Fig. 1 (main text). EMAC results [$\mu g/m^3$(air)]: ISORROPIA II (blue stars), EQSAM4clim (orange circles). The results support our discussion in Sec. 4.1 (main text).

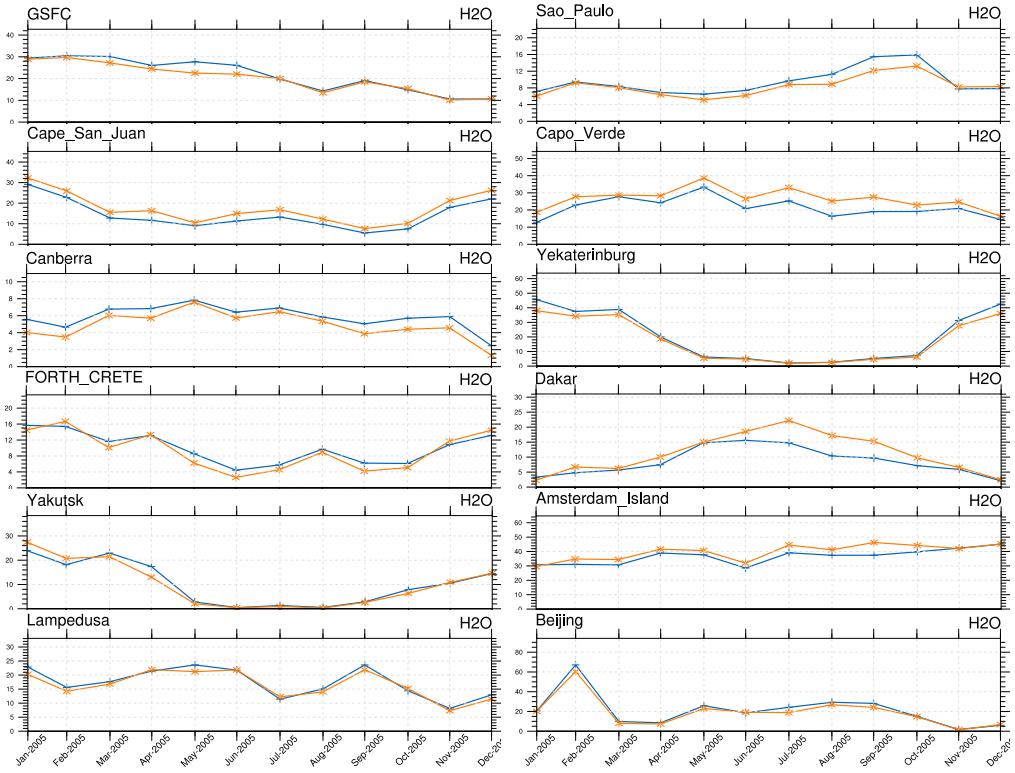

Figure S7: Fig. S6 continued for the total aerosol associated water [$\mu g/m^3$(air)].

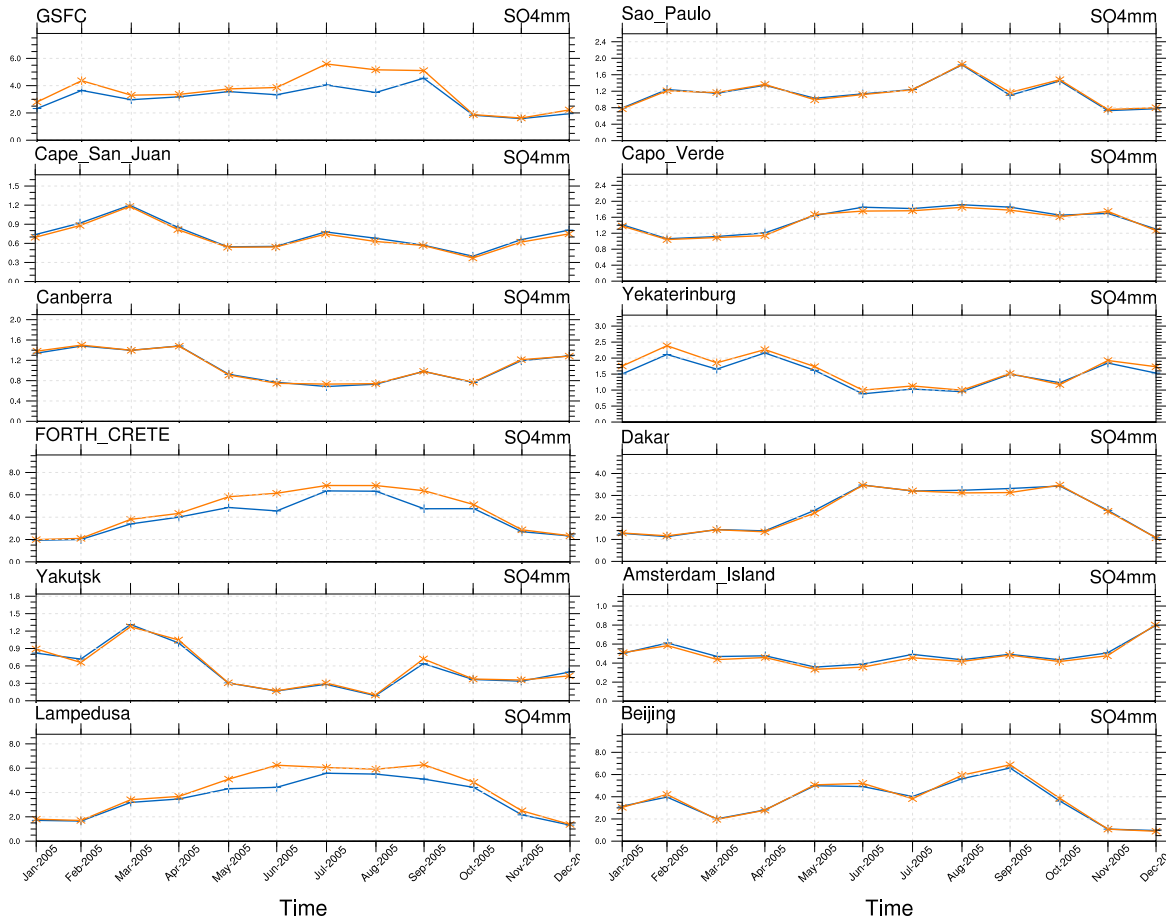

Figure S8: Extension of Figs. S6 and S7. Corresponding EMAC results of lumped sulfate aerosol [$\mu g/m^3$(air)] based on ISORROPIA II (blue stars), EQSAM4clim (orange circles).

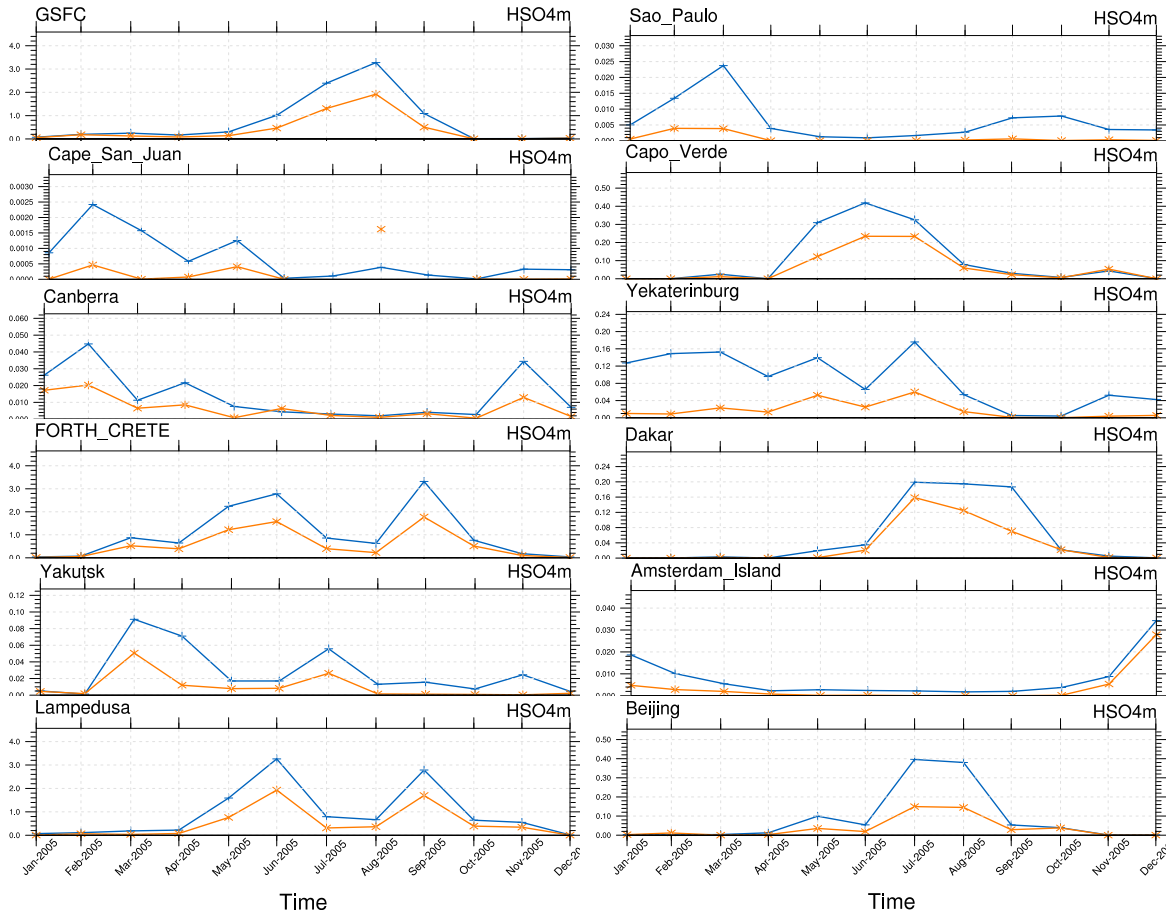

Figure S9: Fig. S8 continued for lumped bi-sulfate aerosol [$\mu g/m^3$(air)].

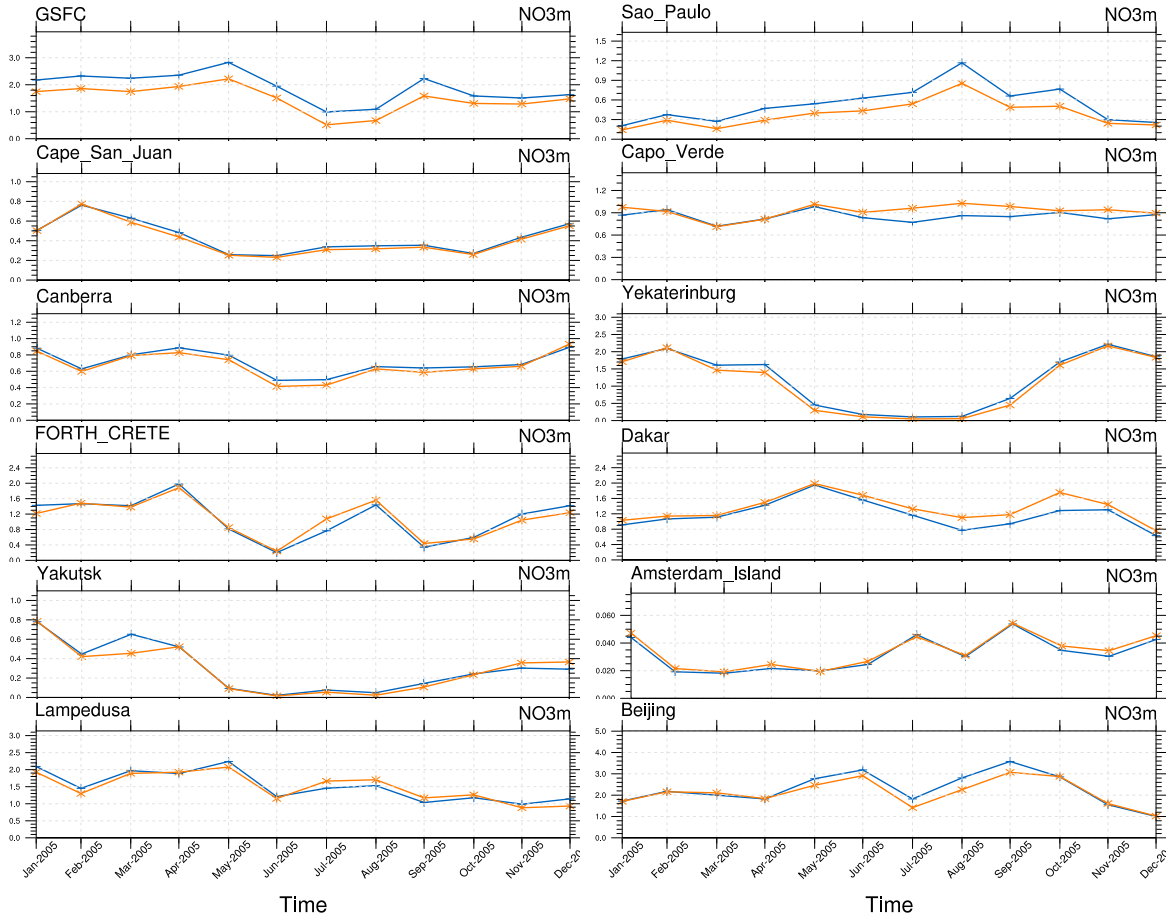

Figure S10: Fig. S8 continued for lumped nitrate aerosol [$\mu g/m^3$(air)].

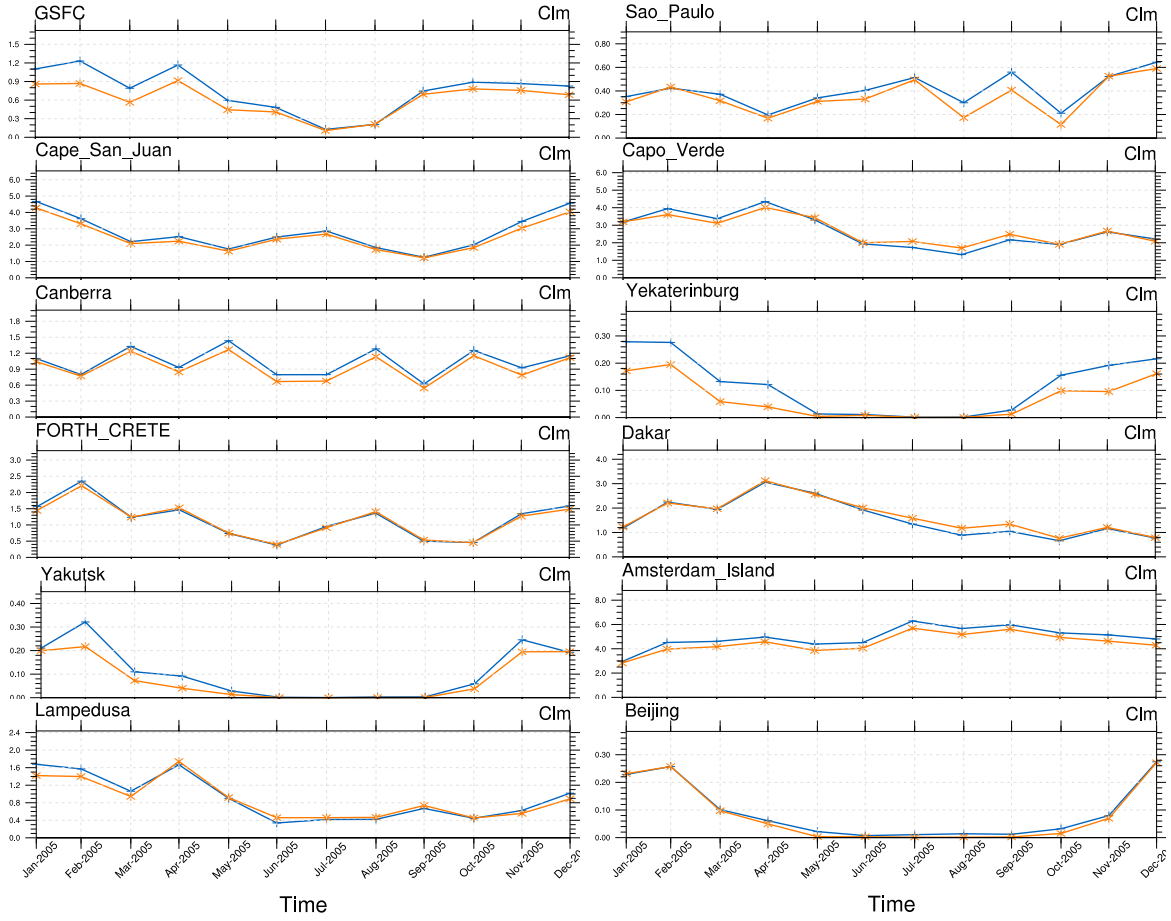

Figure S11: Fig. S8 continued for lumped chloride aerosol [$\mu g/m^3$(air)].

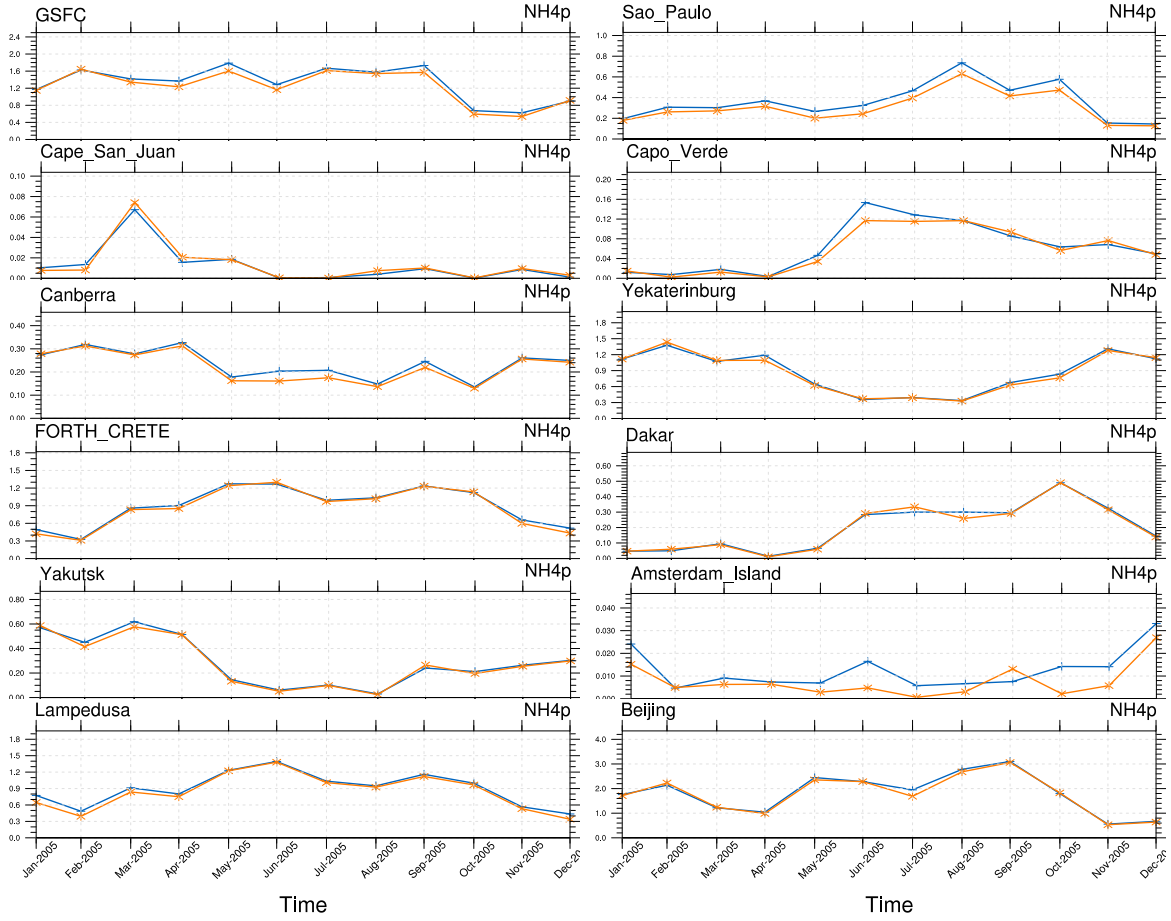

Figure S12: Fig. S8 continued for lumped ammonium aerosol [$\mu g/m^3$(air)].

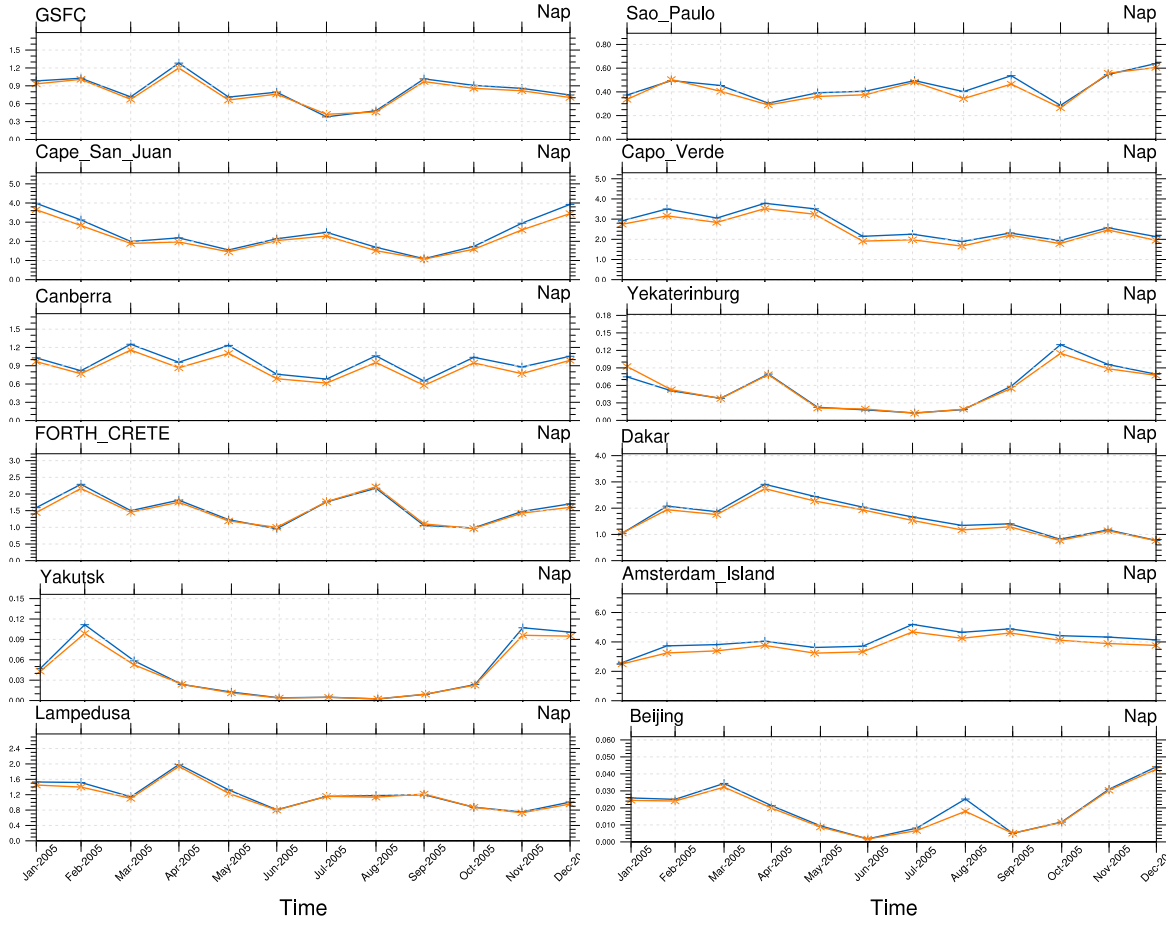

Figure S13: Fig. S8 continued for lumped sodium aerosol [$\mu g/m^3$(air)].

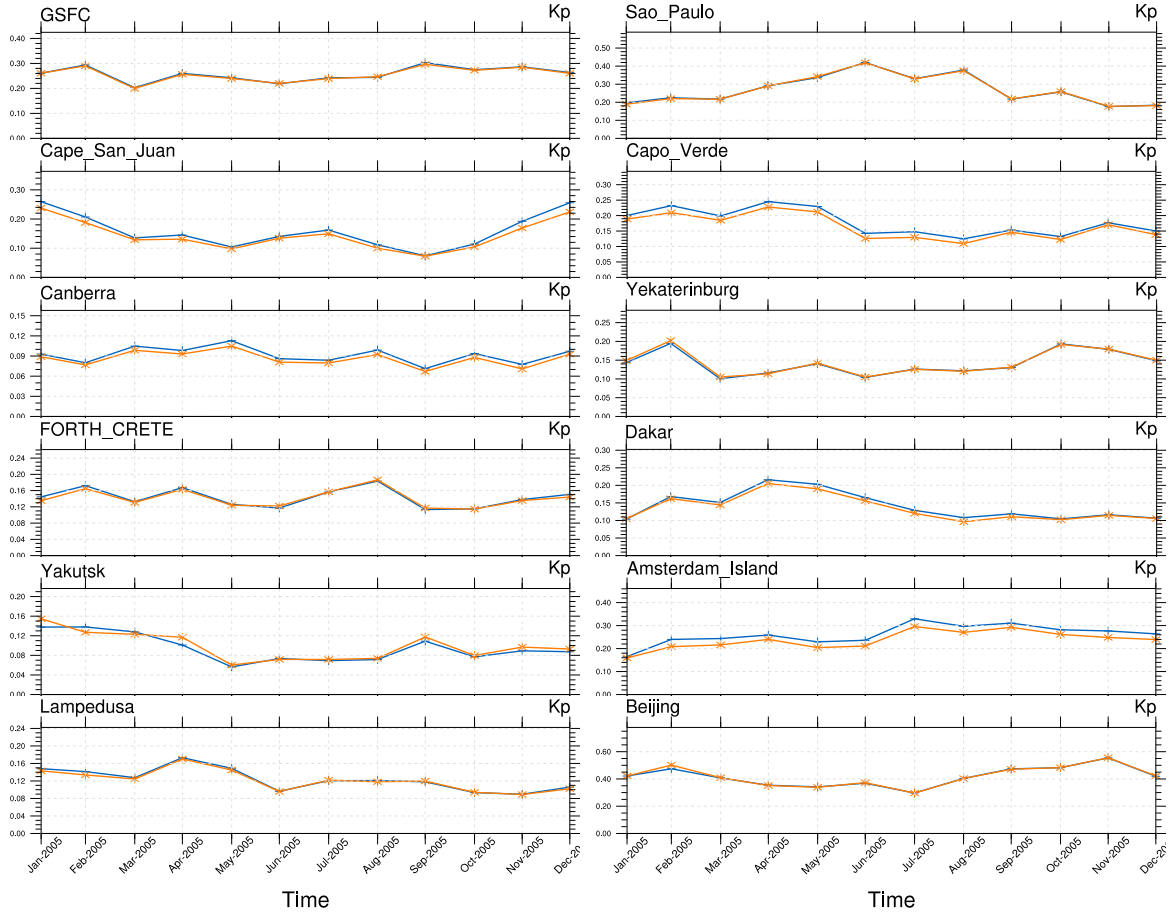

Figure S14: Fig. S8 continued for lumped potassium aerosol [$\mu g/m^3$(air)].

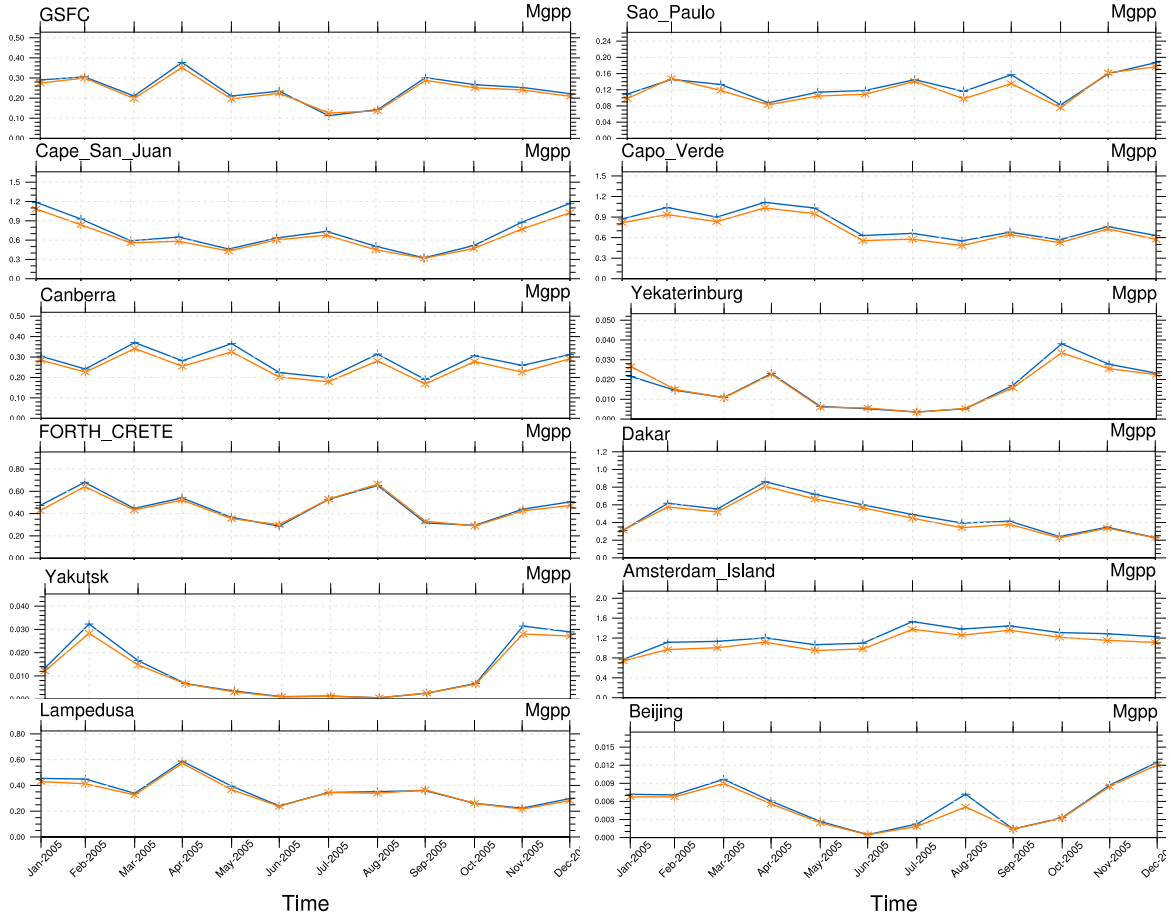

Figure S15: Fig. S8 continued for lumped magnesium aerosol [$\mu g/m^3$(air)].

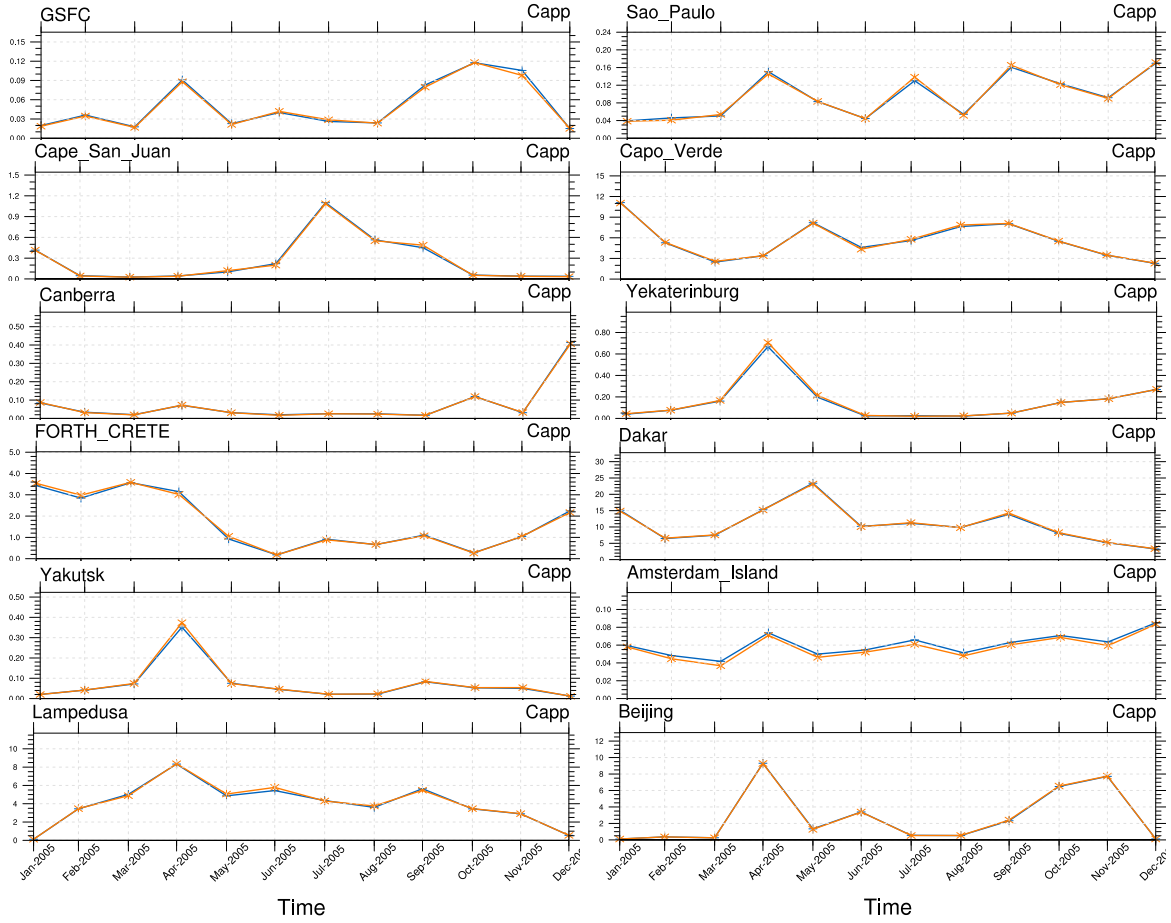

Figure S16: Fig. S8 continued for lumped calcium aerosol [$\mu g/m^3$(air)].

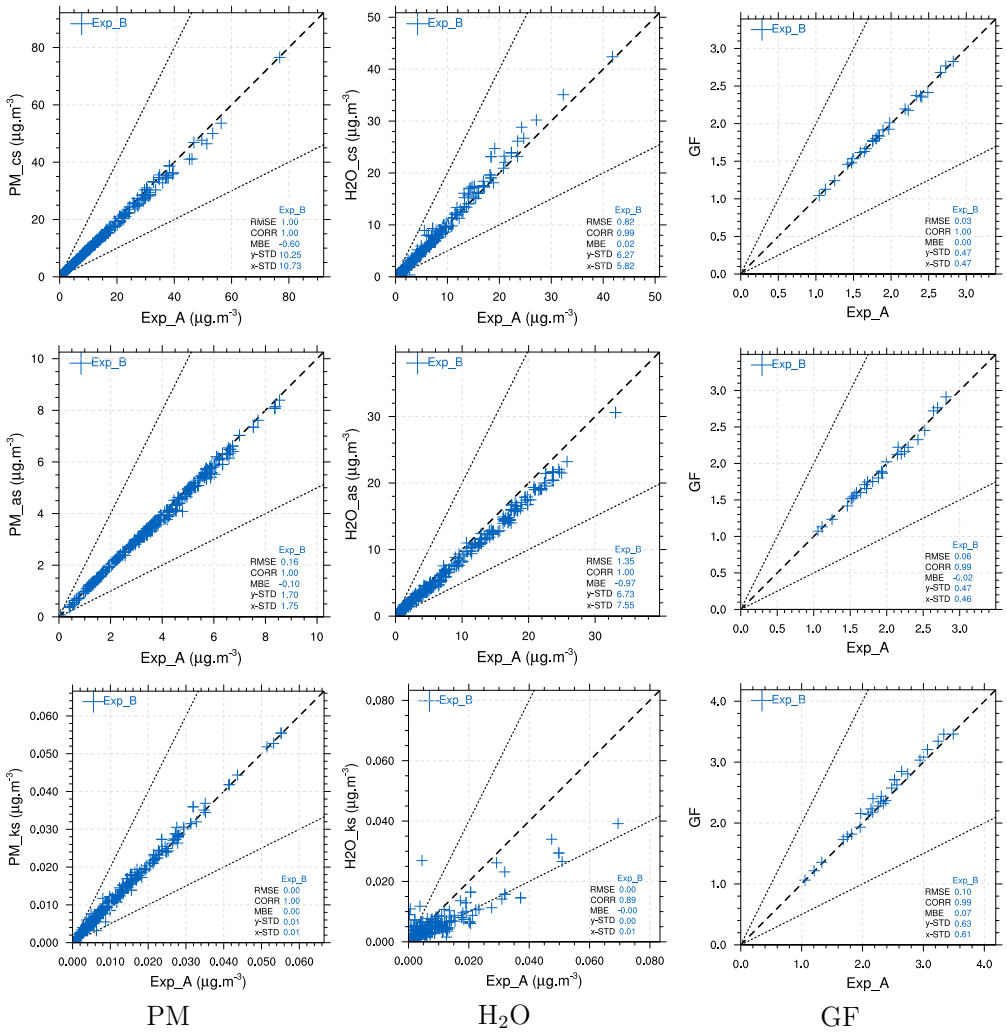

Figure S17: EMAC results based on EQSAM4clim (Exp B, ordinate) versus ISORROPIA II (Exp A, x-ordinate). Results are shown for the total (liquids and solids) particulate matter (left column), aerosol associated water (middle column), associated growth factor (right column). Each scatter plot shows the aerosol coarse mode (top row), accumulation mode (middle row), aitken mode (bottom row) based on monthly mean values (2005) for the 537 AERONET station locations shown in Fig. S1.

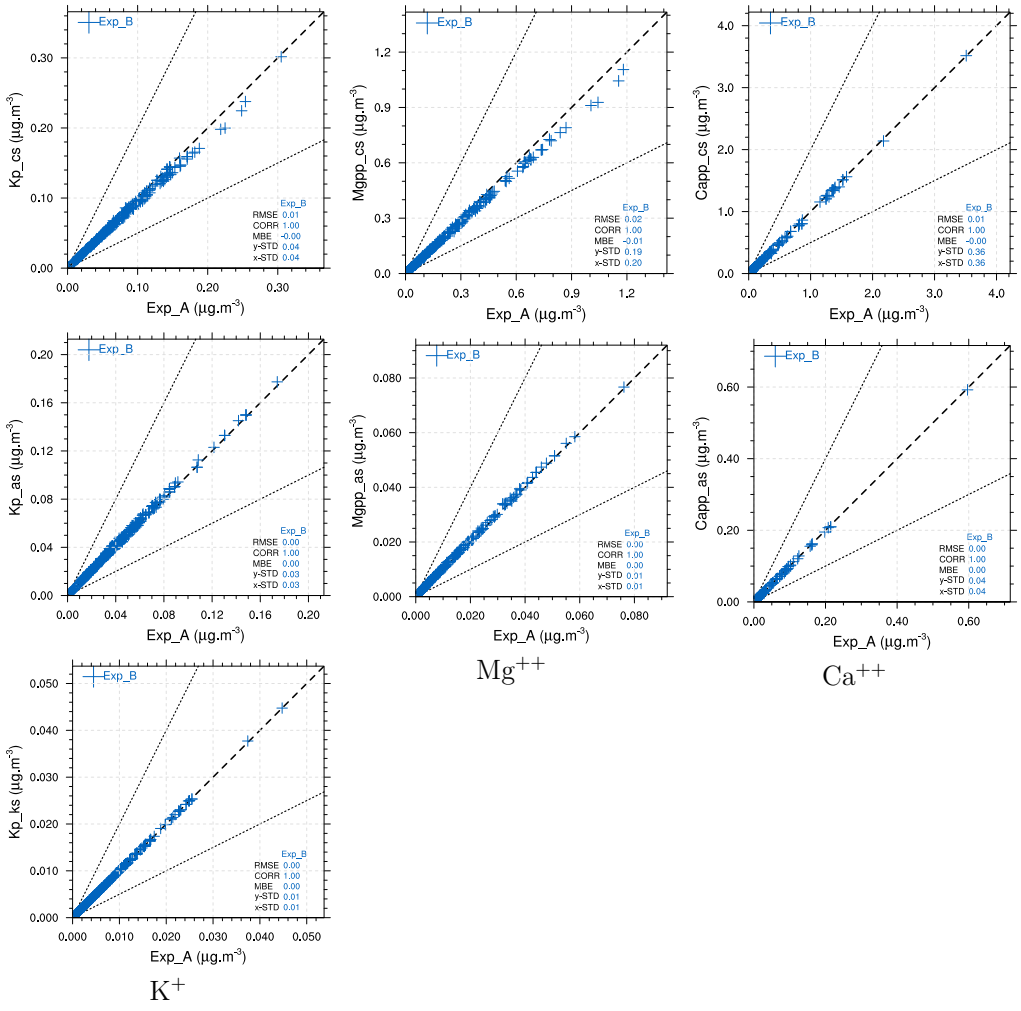

Figure S18: Fig. S17 continued for K^+, Mg^{2+} and Ca^{2+}.

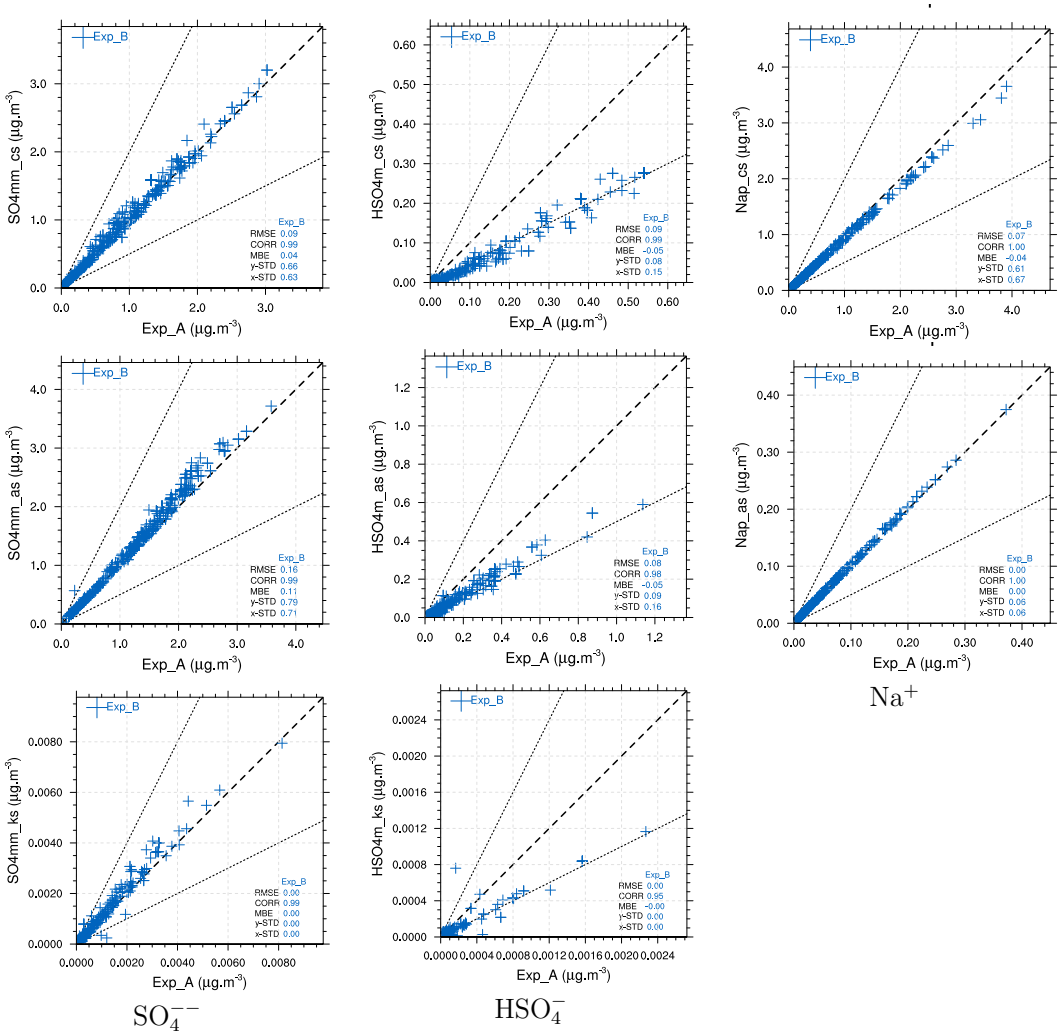

Figure S19: Fig. S17 continued for $SO4^{2-}$, $HSO4^{-}$ and Na^{+}.

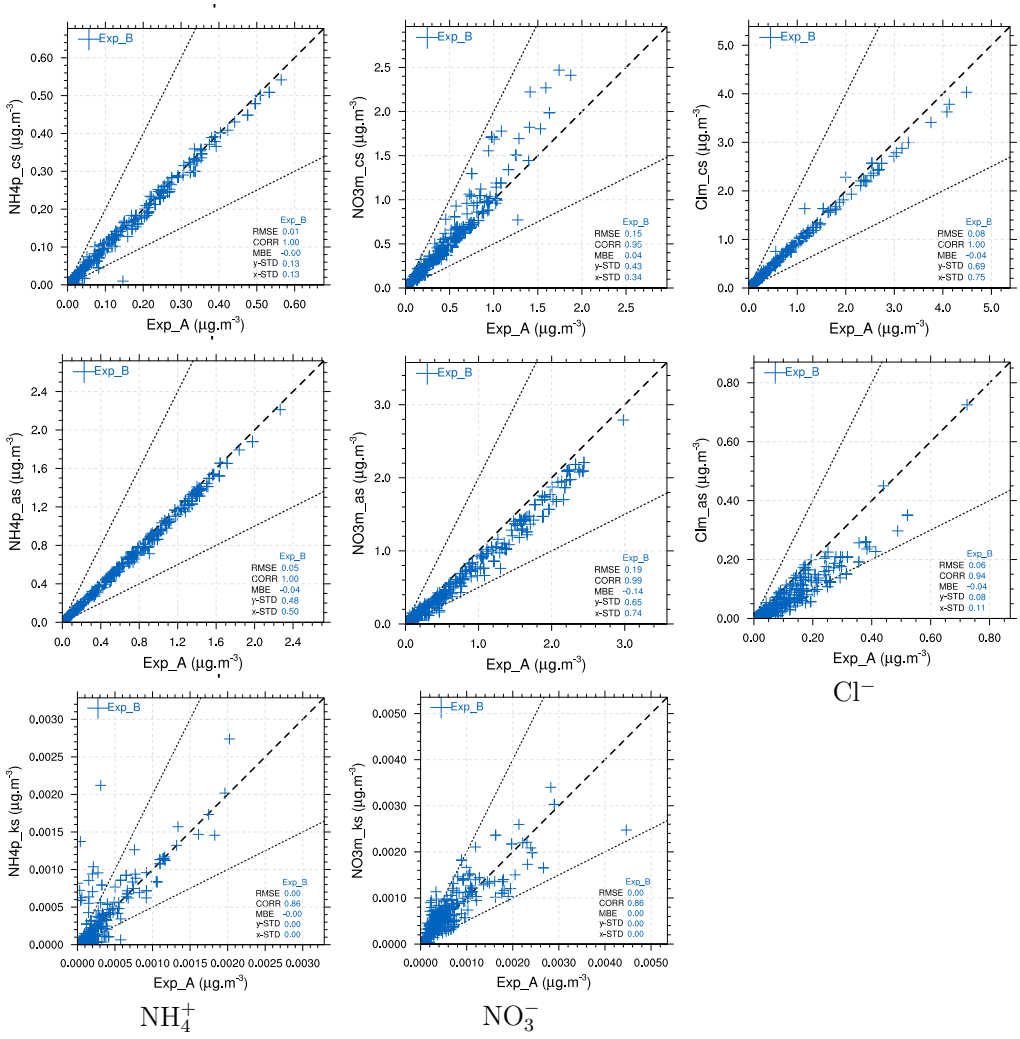

Figure S20: Fig. S17 continued for NH4$^+$, NO3$^-$ and Cl$^-$.